Article

Journal of
Nanoscience and Nanotechnology
Vol. 16, 555–561, 2016
www.aspbs.com/jnn

Recyclable Photo-Thermal Nano-Aggregates of Magnetic Nanoparticle Conjugated Gold Nanorods for Effective Pathogenic Bacteria Lysis

Mohankandhasamy Ramasamy[1], Sanghyo Kim[1], Su Seong Lee[2], and Dong Kee Yi[3, 4, *]

[1] *Department of Bionanotechnology, Gachon University, Seongnam, 461701, Korea*
[2] *Institute of Bioengineering and Nanotechnology, The Nanos, 138669, Singapore*
[3] *Department of Chemistry, Myongji University, Yongin, 449728, Korea*
[4] *Department of Energy and Biotechnology, Myongji University, Yongin, 449728, Korea*

We describe the nucleophilic hybridization technique for fabricating magnetic nanoparticle (MNP) around gold nanorod (AuNR) for desired photo-thermal lysis on pathogenic bacteria. From the electromagnetic energy conversion into heat to the surrounding medium, a significant and quicker temperature rise was noted after light absorption on nanohybrids, at a controlled laser light output and optimum nanoparticle concentration. We observed a similar photo-thermal pattern for more than three times for the same material up on repeated magnetic separation. Regardless of the cell wall nature, superior pathogenic cell lysis has been observed for the bacteria suspensions of individual and mixed samples of *Salmonella typhi* (*S.typhi*) and *Bacillus subtilis* (*B.subtilis*) by the photo-heated nanoparticles. The synthesis of short gold nanorod, conjugation with magnetic nanoparticle and its subsequent laser exposure provides a rapid and reiterated photo-thermal effect with enhanced magnetic separation for efficient bactericidal application in water samples. Resultant novel properties of the nano-aggregates makes them a candidate to be used for a rapid, effective, and re-iterated photo-thermal agent against a wide variety of pathogens to attain microbe free water.

Keywords: Gold Nanorods, Magnetic Nanoparticles, Nano-Aggregates, Photothermal, Pathogen Lysis, Recyclable.

1. INTRODUCTION

Nano scale metals at lower concentrations exhibit microbicidal, bactericidal, fungicidal, and viricidal properties with the advantages of greater surface area and better contact efficiency.[1–5] Particularly gold based materials, due to their inertness and prominent biocompatibility, have been actively involved in various biomedical studies. Having high extinction coefficient and ease of functionalization, gold nanorods (AuNRs), due to their electromagnetic interaction in the visible and NIR regions, have shown significant potential for optical imaging, sensing and drug or DNA deliveries.[6–12] Interestingly, AuNRs acts as a promising photo-thermal agent for effective destruction of cells and tumor tissues.[13–16] AuNRs, work as a targeted hyperthermal agent with the attached antibodies to produce specific cellular damage after laser irradiation.[17–19]

Hybridizing different nanomaterials, imaging, NIR photo-heating, and magnetic properties in each nanocomposite are a platform for simultaneous bio-labeling, cell separation, and photo-thermal application.[20–24] Therefore, the development of single recyclable photo-thermal agents could bring novel opportunities in bio-medical and ecological treatments.

Recently, emerging multi-drug resistant microbial agents are causing severe waterborne diseases and are a major threat to human life.[25–27] The conventional disinfection technologies produce undesirable health issues by producing carcinogenic and mutagenic by-products.[28, 29] So, engineering nanoparticles and applying them without any fluidic attachment for recyclable bacteria lysis are the next generation of exploration in eco-friendly water sanitization.[30, 31] At the same time, easy collection and reuse of the nanomaterials will attain more importance in order to minimize the eco-toxicological issues.

*Author to whom correspondence should be addressed.

In this work, we describe a fresh hybridization of surface functionalized magnetic nanoparticles over a gold nanorod (*hereafter termed as AuNR-MNP aggregates*) with tunable optical and magnetic effects. The AuNR-MNP aggregates subsequently introduced with diode laser, optically induce temperature increasing efficiency to destroy the highly virulent pathogens. Until now, few studies have been conducted for opto-thermal bactericidal effect of AuNR-MNP conjugates with laser.[22, 23] Herein, we are reporting freshly fabricated AuNR-MNP aggregates for highly effective, well repeatable photo-thermal destruction of bacteria at minimal laser energy.

2. EXPERIMENTAL SECTION

AuNRs were prepared as outlined in previous research reports with modifications.[32, 33] The silica coating was accomplished with an ethanolic solution of 10 mM 3-mercaptopropyl trimethoxysilane (MPTMS, Sigma-Aldrich, USA) for 12 h under gentle stirring at pH 9 (with ammonium hydroxide). Purified silica coated AuNRs were added to react with *N*-ethyldiisopropylamine (N-EDIPA, Alfa Aaesar) next to 5,6-epoxyhexyltriethoxysilane (ETES, Gelest Inc. USA) with 100 μl of de-ionized water and were kept on a shaker overnight at room temperature. Un-reacted materials were removed by washing twice with ethanol. Uniform, tetraethylorthosilicate (TEOS, Sigma-Aldrich, USA) capped silica coated MNPs were synthesized as per our previously reported procedure. Prior to silica coating the monodispersed MNPs had been synthesized by the thermal decomposition of iron pentacarbonyl (precursor) in the presence of oleic acid (stabilizer) and octyl ether.[34] For amine immobilization, to the silica coated MNPs, 90 μl ammonium hydroxide was added, followed by 30 μl 3-aminopropyltrimethoxysilane (3-APTMS, Sigma-Aldrich, USA) in ethanol solution and then left to react for 16 h. Amine functionalized MNPs were washed and collected by centrifugation with ethanol. For conjugation, a solution of epoxide functionalized AuNR was added drop-wise to amine MNP in the presence of N-EDIPA and allowed to react on a shaker overnight. Conjugated particles were washed and collected; unattached AuNRs were separated from fabricated AuNR-MNP aggregates by magnet. The purified sample was moved from ethanol to de-ionized water and stored at room temperature for further use.

Differential UV-visible absorption spectroscopy was performed by Varian CARY50 (Varian Inc.). The chemical modifications were studied using Fourier transform infrared spectroscopy (JASCO FT-IR4100) at 4000–400 cm^{-1}. Zeta-potential measurements were taken using a Malvern Zeta-Sizer 3000HS. Morphological characteristics and elemental analysis were studied using field emission scanning electron microscopy (FE-SEM, JEOL Corp., JSM6700F) and high-resolution transmission electron microscopy (HR-TEM-EDS, Tecnai G2TF30ST).

Reproducible photo-thermal efficiency of AuNR-MNP aggregate (20 mg/ml) was examined with DPSS laser (Dream laser system, Japan) with a central wavelength of 671 nm at 130 mW. The temperature difference was recorded with a thermocouple (K type, Omega) interfaced with a data acquisition system (34970, Aglient, CA, USA). To study the photo-thermal effect on bacteria, *S. typhi* and *B. subtilis* (individually and together) mixed with 20 μl nano-aggregate dispersion and then exposed to laser light for 12 min. An external magnet was used to separate the nano-aggregate for multiuse. The resulting clear suspension was drawn out carefully with a pipette and washed once by centrifugation. The resulting pellet was re-suspended in sterile saline. Live/Dead® BacLight™ Bacterial viability kit (Invitrogen) was employed to measure the order of cell death under laser scanning fluorescence microscopy (Nikon Eclipse TE 2000-U). In addition, the cell integrity of the bacteria before and after laser irradiation was recorded using Bio-AFM (Nanowizard II, JPK instruments, Berlin, Germany).

3. RESULTS AND DISCUSSION

The short AuNRs with an aspect ratio of 2.3 were constructed in aqueous solution using a cationic surfactant directed seed-mediated method.[35] CTAB less AuNR was treated with MPTMS for a 12 h mediation process to form Au–SH bonding; the $-Si(OH)_3$ groups extended outward as a protective layer. Subsequent modification is caused by applying the ETES with water to form very thin layer of epoxide ($-CH_2-O-CH_2$) coverage on the exterior surface of silica coated AuNR. N-EDIPA in water acted as an auxiliary base to complete the reaction. MNPs were previously involved in the hydrolysis reaction and subsequent condensation of TEOS in the presence of ammonium hydroxide to form a homogeneous silica shell over the particle for better surface modification. Post synthetic silanization was carried out with 3-APTMS to impart a rich amine outer layer for further conjugation. The source of the amino groups was 3-APTMS molecules, with the chemical formula $H_2N-(CH_2)_3-(OMe)_3-Si$, where –OMe is a hydrolysable part used for the adhesion to the silica coated MNP surface with a –O–Si–O– network. The extending alkyl chain ends with the amino groups which control the reaction conditions by controlling the surface concentration on the nanoparticles. Epoxide functionalized AuNRs were hybridized with the amine groups in the MNPs by undergoing nucleophilic reaction (Fig. 1), which allows the ring at the electrophilic epoxide carbon to open and fuse together.[36] Basically, amine groups attack the less substituted epoxide carbon to yields secondary alcohol.[37] The attaching ratio of MNPs over AuNRs can be controlled by changing the quantity of nanoparticles and their method of application. In contrast to the existing methods, we report here for the first time a better conjugation

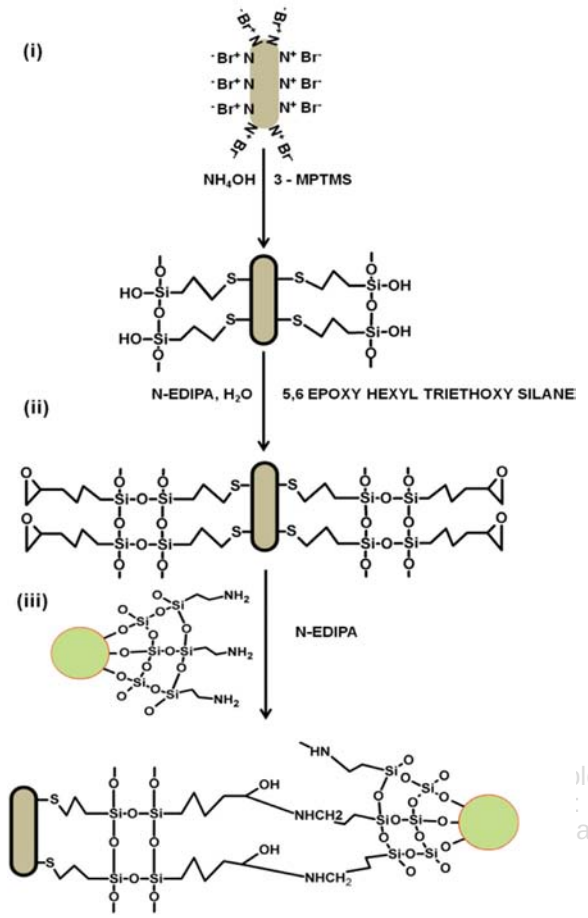

Figure 1. Surface chemistry involved in the hybridization of MNP with AuNR. (i) Synthesis of silica coated AuNR using 3-mercaptopropyl trimethoxysilane (MPTMS), (ii) surface modification of silica coated AuNR with epoxide ring with the help of N-ethyldiisopropylamine (N-EDIPA), and (iii) nucleophilic conjugation between amine ends of MNP with AuNR after epoxide ring cleavage.

technique of nucleophilic hybridization between two different nanoparticles (AuNR and MNP).

Figures 2(a)–(c) shows the FE-SEM images of bare, silica coated, and epoxide coated AuNRs. The images clearly indicating that AuNRs after surface modification became highly dispersive compare to the uncoated AuNRs. The inset (c″) depicts the enlarged view of the AuNR with a distinct layer from the core surface which confirms the successful functionalization of the AuNR surface. The UV-Vis/NIR spectrum of AuNRs was characterized by distinct peaks at 520 nm and 650 nm for its short and longitudinal surface plasmon resonance upon light absorption (Figs. 2(a′)–(c′)). In addition, AuNRs show alteration in their optical properties after surface modification. Thus, shifts of 6 and 16 nm in the longitudinal peak were observed for silica coated AuNRs and epoxide coated AuNRs, respectively; confirming the formation of new layers on the surface. Figures 2(d) and (e) depicts the MNPs before and after surface modification. The high resolution image in the inset (Fig. 2(e′)) clearly indicates the formation and complete covering of individual nanoparticles by a uniform silica layer with improved distribution. Figure 2(f) shows the hybridization of two different surface modified nanoparticles. The enlarged view of the AuNR-MNP aggregate in the inset (Fig. 2(f′)) confirms the successful conjugation between nanoparticles. Due to hybridization, the MNPs attracted toward AuNR, thus formed a highly crowded MNP around AuNR, forming aggregates. From the image (Fig. 2(f′)) it is clearly visible that the amine functionalized MNP showed tight conjugation with more particles near or around the AuNRs surface whereas the un-conjugated MNPs scattered in the distance. In conjunction, to confirm our method of conjugation, the long AuNRs were also utilized which were made hybridized with surface modified MNP by the same nucleophilic hybridization mechanism and the corresponding microscopy images are presented in the Figure 3. These results also corroborate the successful nucleophilic hybridization between nanoparticles. Figure 3 depicts the conjugation of MNP towards the entire AuNR surface. Hence, immediate collection and repeated usage of nanohybrids might be possible for multiple photothermal cycles of nanohybrids without appreciable loss.

Qualitative verification using FT-IR confirms the 3-APTMS grafting onto the silica coated MNPs and its successful conjugation with AuNRs (Fig. 4(a)). O–H stretching vibration at 3450 cm^{-1}, N–H stretch at 3100–3300 for secondary amine, and C–N stretch around 1150 cm^{-1} confirmed AuNR-MNP conjugation. In addition, the disappearance of the epoxide group band at 910 cm^{-1} confirmed the ring opening and its fusion with the amine group at the nucleophilic level.[38] The zeta potential values of −28 mV and −30.6 mV for silica coated AuNR and MNP became +21.4 mV and +25.3 mV after surface modification with epoxide and amine functionalities, respectively. These high values support successful surface alteration with good colloidal stability.

The magnetic collection of AuNR-MNP aggregate after photothermal treatment against bacteria suspension is shown in Figure 4(b). Initially the conjugated nanoparticles in water show slow attachment towards external magnet (Figs. 4(b b′)). But after the laser irradiation with bacteria, magnetic collection was quicker (Figs. 4(b), (d′)). Highly improved capture efficiency with a handheld magnet is observed due to the MNPs that are densely attached to the AuNRs and the quick aggregation of particles in saline solution.

AuNRs are photo-thermal agents, which convert photons into heat by non-radiative processes.[39] Due to surface plasmonic resonance of AuNRs, the crystal lattice is heated via electron–phonon interaction and is cooled by transporting its heat to the surrounding medium via

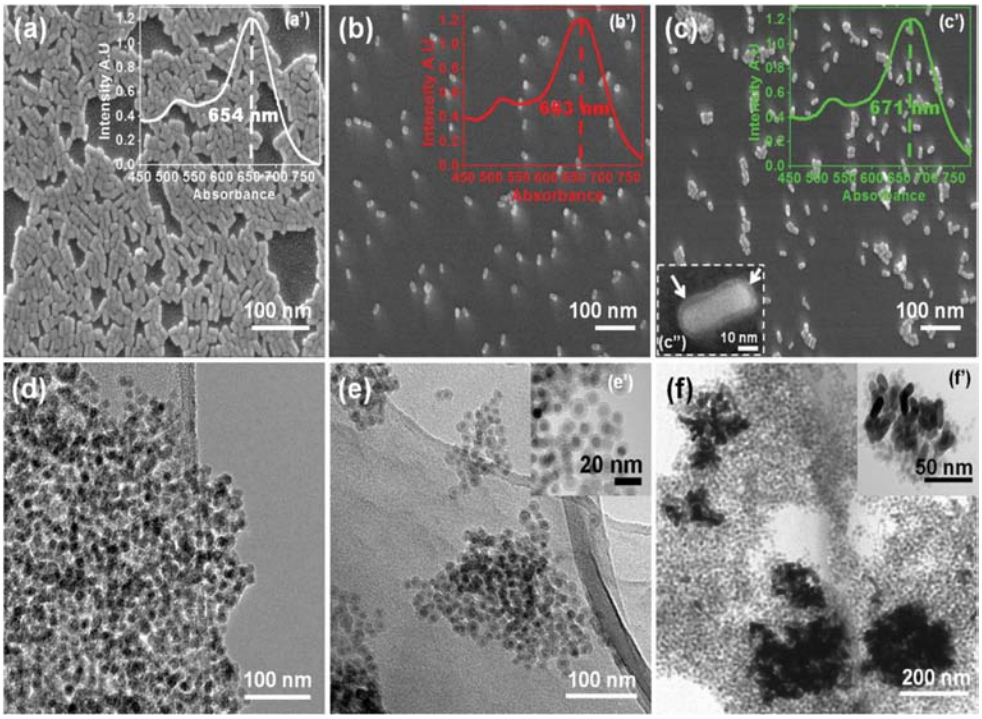

Figure 2. FE-SEM images of uncoated AuNRs (a), silica coated AuNRs (b), and epoxide-coated AuNRs (c) and their corresponding UV-Vis spectra as (a′), (b′), and (c′). The inset (c″) is a high magnification image with distinct thin epoxide layer around AuNR which can be distinguished from the core. HR-TEM micrographs of MNPs (d), silica coated MNPs (e), and AuNR-MNP conjugates (f). The inset (e′) is the enlarged view of silica coated MNPs and (f′) is the single AuNR-MNP aggregate.

phonon–phonon relaxation on a picosecond time scale.[13–15] The photo-thermal effect was accomplished by matching the laser excitation wavelength to the longitudinal surface plasmon resonance of AuNR.[40] Figure 5 shows the reiterated photo-thermal response of the light exposed AuNR-MNP aggregate. Laser light on water causes negligible temperature change and MNPs heated to 42 °C, which is not enough to do irreparable cellular damage to bacteria. On the other hand, AuNR-MNP shows a sharp increase in temperature of 45 °C within seconds. Further, the maximum of 70 °C was reached in just 12 min; then there was no change in temperature even extending laser exposure up to 15 min. These water soluble nanohybrids made with silica coated AuNRs were found to have more repeatable photo-thermal response than bare AuNR. The uncoated AuNR does not show or withstand consistent temperature rise due to the Ostwald ripening shape deformation (from rod to spherical) on exposure to high temperature.[41,42] But the silica coated rod's temperature keeps rising after continuous laser illumination because the silica layer on the rod slows down the Ostwald ripening and restrains the shape changes which maintain both longitudinal and transverse width. Most importantly, as exhibited AuNR-MNP nano-aggregate to laser can be easily recovered by a magnet, and they could be recycled up to 6 times without metal leaching from the nanohybrid. In general, nanomaterials have the disadvantages of being relatively toxic to humans and the environment, being difficult to recollect once dispersed, and being expensive if not re-used. In contrast, our synthesized nano-aggregates can be easily recovered and are recyclable without any loss, which makes it them more economical and eco-friendly.

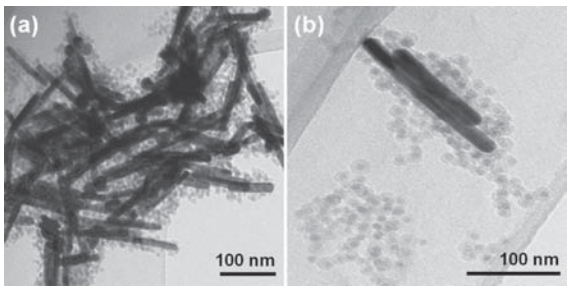

Figure 3. (a) FT-IR spectra of (a) Epoxide AuNRs, (b) amine functionalized MNPs, and (c) AuNR-MNP conjugated nanohybrid. (b) AuNR-MNP aggregate dispersion in water (a′), collection of the nano-aggregate with permenant magnet in water before laser illumination (without bacteria) (b′), Photothermal therapy on AuNR-MNP aggregate dispersed bacteria suspension with continuous laser exposure, the temperature change was monitored with the aid of thermocouple (c′), and the collection of laser irradiated AuNR-MNP aggregate from bacteria suspension in saline for reuse of the same material (d′).

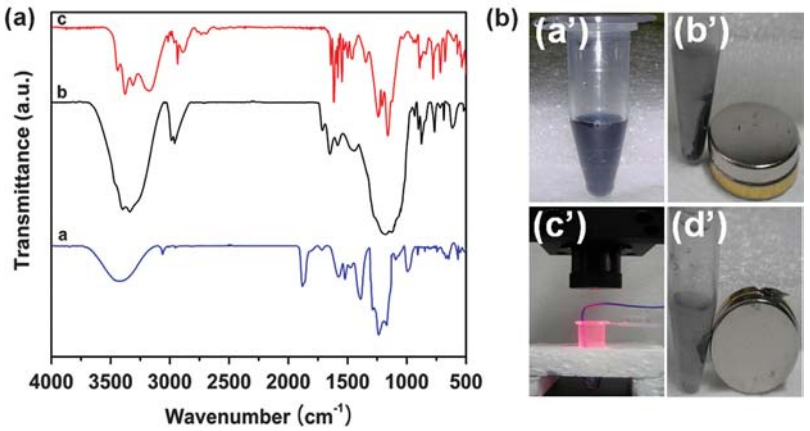

Figure 4. Conjugation efficiency of different nanoparticle. HR-TEM images epoxide functionalized long AuNR conjugated with amine modified MNP (a) and its magnified view (b).

Optothermal cell lysis was examined to determine the anti-bacterial property of the nano-aggregate after laser irradiation. Added saline enables quick precipitation and ease of magnetic tracking efficiency for nano-aggregates from the suspension. The dye kit (SYTO9 and propidium iodide) was used to determine the rate of bacteria lysis from the images of fluorescence microscopy (Fig. 6). SYTO9, the membrane permeant dye, enters into bacteria and stains DNA to produce green fluorescence in living bacteria. On the other hand, propidium iodide labeling shows dead bacteria with red fluorescence due to the damage in cell wall by thermolysis. Representative fluorescence microscopy images (Fig. 6) clearly demonstrate the viability/mortality rates of single and mixed bacteria samples. The laser alone caused negligible cellular damage. The combined effect of AuNR-MNP aggregate with laser on bacteria caused photothermal destruction of the cellular population. Interestingly, compared to single bacteria samples, the mixed bacteria showed superior cell lysis without a single surviving bacteria. As shown in Figure 6, the image was filled entirely with red fluorescence of dead bacteria without any green fluorescence of live cells. Further the Bio-AFM was adopted to analyze the morphological changes that occurred in the bacteria (*S.typhi*) before and after laser illumination. Figure 7(a) illustrates that the controlled bacteria had organized smooth surface with proximity in population. In contrast, the photothermally exposed bacteria exhibited significant shape alterations including disorganized and broken structure in Figure 7(b). Furthermore, the micrograph clearly depicts the disoriented shape of the bacteria and the serious irrevocable damage to the cells. The photo responsive effect by the AuNR-MNP aggregate in the presence of the laser at tuned wavelength caused irreparable cellular damage to the bacteria regardless of its cell wall composition. The only possible mechanism for the cell lysis could be the photothermal effect of AuNR present in the AuNR-MNP aggregate. The exact principle of the cell disintegration and its molecular level mechanism toward photothermal effect are yet to be realized. Previous research reported that synthesized nanoparticle suspension produces a maximum temperature of 55 °C with 2 min of NIR laser irradiation is a photo-thermally efficient material against bacteria, without considering the factor of toxicity.[43] In our method, the synthesized silica coated AuNRs, which had previously been reported as non-toxic,[44] strongly demonstrate that the bacterial lysis developed due to the nanohybrid and laser interaction rather than the toxicity of nanoparticles. All together, the resulting photo-thermal ability of our AuNR-MNP to affect the pathogens makes these nano-aggregates highly effective for the potential removal of different bacteria from water. Further, this nanotechnology based method could be intended to remove other disease

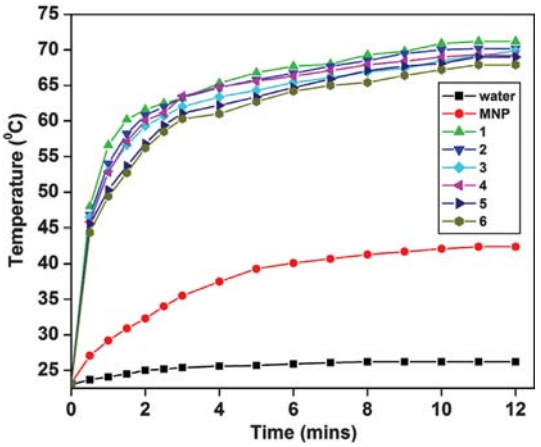

Figure 5. The re-iterated photo-thermal responses of a magnetically recollected single concentration AuNR-MNP aggregate with a continuous laser exposure at 12 min along with light irradiated MNPs temperature change.

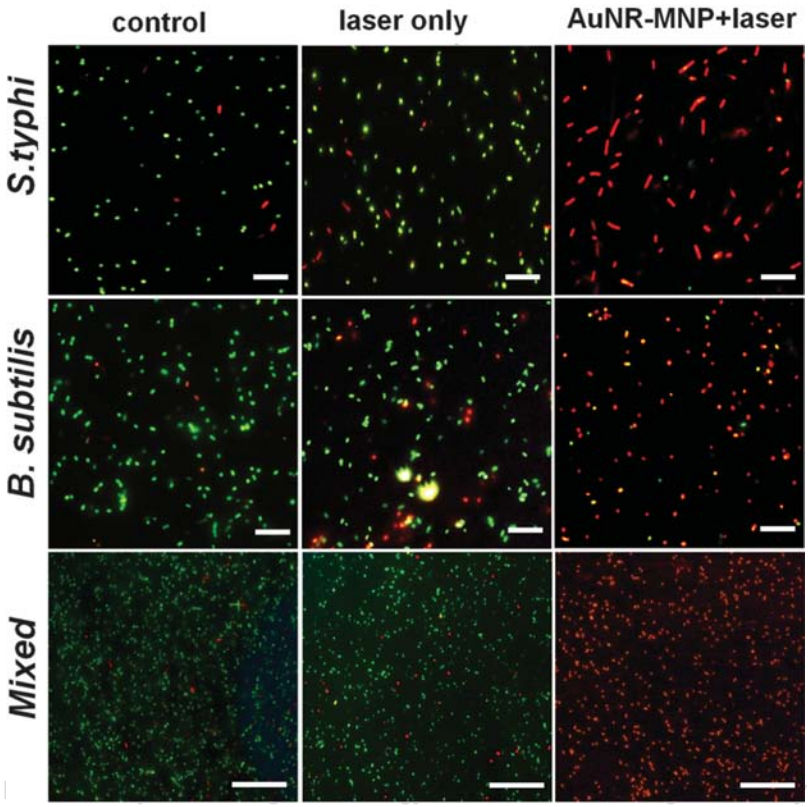

Figure 6. Fluorescence microscopy images of separate and mixed strains of *S. typhi* and *B. subtilis* after laser exposure at 130 mW for 12 min. Green fluorescence indicates live cells while red fluorescence represents dead cells at 50× magnification for individual bacteria and 20× for mixed bacteria samples.

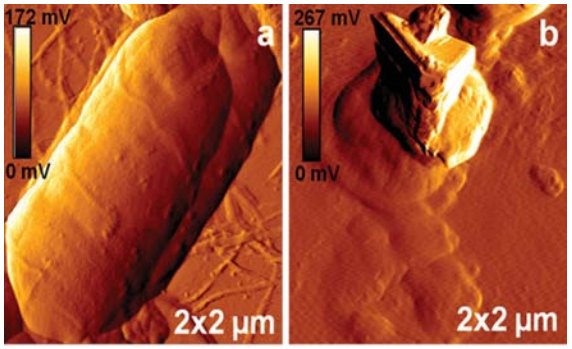

Figure 7. Bio-AFM micrographs of (a) controlled *S. typhi* with integrated cell membrane, and (b) destroyed bacteria, cell membrane shrinkage and with effluent cytoplasm.

causing microbes as well, to make pathogen free water in a quicker time.

4. CONCLUSION

We reported a unique initial step of a nanotechnology adopted technique for the nucleophilic level hybridization of epoxide gold nanorods with amine covered magnetic nanoparticles. The most promising aspects of the synthesized AuNR-MNP aggregates are; wide range of pathogen lysis, photo-thermal recyclability without loss, easy collection, economical, and eco-friendly which makes them a suitable candidate for real world applications. From the combination of engineered nanohybrids and laser light, and its produced photo-thermal behavior, we have successfully achieved a complete destruction of bacterial pathogens in water samples. We believe this approach may be used as a better strategy for providing recyclable bacteria eradication from water in short time so they can be applied to other types of microbes as well.

Acknowledgment: This research was supported by Korean NRF, NRF-2013R1A1A2005329.

References and Notes

1. J. Keleher, B. Bashant, N. Heldt, L. Johnson, and Y. Li, *World J. Microbiol. Biotechnol.* 18, 133 **(2002)**.
2. Z. Lu, C. M. Li, H. Bao, Y. Qiao, Y. Toh, and X. Yang, *Langmuir* 24, 5445 **(2008)**.
3. S. Kang, M. Herzberg, D. F. Rodrigues, and M. Elimelech, *Langmuir* 24, 6409 **(2008)**.
4. J. Ramyadevi, K. Jeyasubramanian, A. Marilani, G. Rajakumar, and A. A. Rahuman, *Mat. Lett.* 71, 114 **(2012)**.

5. R. S. Norman, J. W. Stone, A. Gole, C. J. Murphy, and T. L. Sabo-Attwood, *Nano Lett.* 8, 302 **(2008)**.
6. D. K. Yi, I. C. Sun, J. H. Ryu, H. Koo, C. W. Park, and I. C. Youn, *Bioconjug. Chem.* 21, 2173 **(2010)**.
7. L. Cognet, S. Berciaud, D. Lasne, and B. Lounis, *Anal. Chem.* 80, 2288 **(2008)**.
8. C. Sönnichsen and A. P. Alivisatos, *Nano Lett.* 5, 301 **(2005)**.
9. C. Yu and J. Irudayaraj, *Anal. Chem.* 79, 572 **(2007)**.
10. C. J. Murphy, A. M. Gole, S. E. Hunyadi, J. W. Stone, P. N. Sisco, and A. Alkilany, *Chem. Commun.* 5, 544 **(2008)**.
11. T. Kawano, Y. Niidome, T. Mori, Y. Katayama, and T. Niidome, *Bioconjug. Chem.* 20, 209 **(2009)**.
12. C. C. Chen, Y. P. Lin, C. W. Wang, H. C. Tzeng, C. H. Wu, and Y. C. Chen, *J. Am. Chem. Soc.* 128, 3709 **(2006)**.
13. S. Link and M. A. El-Sayed, *Int. Rev. Phys. Chem.* 19, 409 **(2000)**.
14. X. Huang, P. K. Jain, I. H. El-Sayed, and M. A. El-Sayed, *Lasers Med. Sci.* 23, 217 **(2008)**.
15. M. A. El-Sayed, *Acc. Chem. Res.* 34, 257 **(2001)**.
16. W. Jo, K. Freedman, D. K. Yi, R. K. Bose, K. K. Lau, S. D. Solomon, and M. J. Kim, *Biofabrication* 3, 015002 **(2011)**.
17. C. A. Peng and C. H. Wang, *Cancers* 3, 227 **(2011)**.
18. C. B. Kim, D. K. Yi, P. S. Kim, W. Lee, and M. J. Kim, *J. Nanosci. Nanotechnol.* 9, 2841 **(2009)**.
19. S. Wang, A. K. Singh, D. Senapati, A. Neely, H. Yu, and P. C. Ray, *Chemistry* 16, 5600 **(2010)**.
20. A. Gole, J. W. Stone, W. R. Gemmill, H. C. zur Loye, and C. J. Murphy, *Langmuir* 24, 6232 **(2008)**.
21. U. Tamer, Y. Gundogu, I. H. Boyaci, and K. Pekmez, *J. Nanpart. Res.* 12, 1187 **(2010)**.
22. C. Wang and J. Irudayaraj, *Small* 6, 283 **(2010)**.
23. U. Tamer, I. H. Boyac, E. Temur, A. Zengin, I. Dincer, and Y. Elerman, *J. Nanopart. Res.* 13, 3167 **(2011)**.
24. M. Ramasamy, S. S. Lee, D. K. Yi, and K. Kim, *J. Mater. Chem. B* 2, 981 **(2014)**.
25. S. E. Hrudey and E. J. Hrudey, *Water Environ. Res.* 79, 233 **(2007)**.
26. M. Leeb, *Nature* 431, 892 **(2004)**.
27. S. R. Norrby, C. E. Nord, and R. Finch, *Lancet. Infect. Dis.* 5, 115 **(2005)**.
28. J. H. Calhoun, J. A. Cobos, and J. T. Mader, *Orthoped. Clin. NA* 22, 467 **(1991)**.
29. Q. Li, S. Mahendra, D. Y. Lyon, L. Brunet, M. V. Liga, and D. Li, *Water Res.* 42, 4591 **(2008)**.
30. M. Veerapandian, S. Sadhasivam, J. Choi, and K. Yun, *Chem. Eng. J.* 209, 558 **(2012)**.
31. M. Veerapandian, L. Zhang, K. Krishnamoorthy, and K. Yun, *Nanotechnology* 24, 395706 **(2013)**.
32. B. Nikoobakht and M. A. El-Sayed, *Chem. Mater.* 15, 1957 **(2003)**.
33. T. K. Sau and C. J. Murphy, *Langmuir* 20, 6414 **(2004)**.
34. D. K. Yi, S. S. Lee, G. C. Papaefthymiou, and Y. Jackie, *Chem. Mater.* 18, 614 **(2006)**.
35. N. R. Jana, L. Gearheart, and C. J. Murphy, *J. Phys. Chem. B* 150, 4065 **(2001)**.
36. A. Rosowsky, The Chemistry of Heterocyclic Compounds, Part 1, Interscience Publishers, New York **(1964)**, Vol. 19, p. 1.
37. B. Ellis, Chemistry and Technology of Epoxy Resins, Blackie Academic and Professional, Glasgow **(1993)**, p. 117.
38. C. Tarducci, E. J. Kinmond, and J. P. S. Badyal, *Chem. Mater.* 12, 1884 **(2000)**.
39. L. Tong, Q. Wei, A. Wei, and J. X. Cheng, *Photochem. Photobiol.* 85, 21 **(2009)**.
40. S. Mallick, I. C. Sun, K. Kim, and D. K. Yi, *J. Nanosci. Nanotechnol.* 13, 3223 **(2013)**.
41. C. Gautier, A. Cunningham, L. Si-Ahmed, G. Robert, and T. Burgi, *Gold Bulletin* 43, 94 **(2010)**.
42. R. Zou, Q. Zhang, Q. Zhao, F. Peng, H. Wang, H. Yu, and J. Yang, *Colloids Surf. A* 372, 177 **(2010)**.
43. W. C. Huang, P. J. Tsai, and Y. C. Chen, *Small* 5, 51 **(2009)**.
44. D. K. Yi, *Mater. Lett.* 65, 2319 **(2011)**.

Received: 8 July 2014. Accepted: 16 September 2014.